

STEPWISE STRESS TESTING OF DIFFERENT CAD/CAM LITHIUM-DISILICATE
VENEER APPLICATION METHODS TO LITHIUM-DISILICATE
SUBSTRUCTURE

by

Jaren Thomas May

Submitted to the Graduate Faculty of the School of
Dentistry in partial fulfillment of the requirements
for the degree of Master of Science in Dentistry,
Indiana University School of Dentistry, 2019.

Thesis accepted by the faculty of the Departments of Cariology and Dentistry and Dental Public Health, Indiana University School of Dentistry, in partial fulfillment of the requirements for the degree of Master of Science in Dentistry.

Kim Diefenderfer

Sabrina Feitosa Sochaki
Chair of the Research Committee

N. Blaine Cook
Program Director

Date

ACKNOWLEDGMENTS

This thesis is dedicated to my wife, Jo Anne, my son, Jacek, and my daughter, Jiana for their constant support and understanding throughout this master's program.

This thesis is also dedicated to my parents for their constant support resulting in the belief that goals are attainable. Their desire to impress on me belief in self, a love of learning and an appreciation for the value of education have made this achievement possible.

This project is only possible with the support of many people. I would like to especially thank my mentor, Dr. Sabrina Feitosa Sochaki, for her patient guidance, support, and for always treating me as a colleague throughout this entire project and the other studies we have conducted.

I would also like to thank Dr. Kim Diefenderfer for helping me to think through the details and be sure that my study is as reproducible and relevant as possible prior to starting.

I would like to thank Dr. N. Blaine Cook for his constant support and willingness to entertain my unending ideas throughout this project and my entire residency. It is amazing what someone can accomplish with the appropriate amount of understanding and guidance from their leaders.

I thank Mr. George Eckert and Mr. Qing Tang for providing their experience and statistical expertise.

I thank Dr. Anelyse Arata for helping us with the complex calculations that were necessary for this project.

I am grateful to the fantastic imaging assistance we were given by Caroline Miller and her lab at the IU School of Medicine Electron Microscopy Center

Special thanks to Ms. Abby Morgan for sharing her wonderful visual talents and aiding us with our graphs and tables so people will want to read them.

I would like to especially thank Mrs. Judy Haines for being a constant and memorable presence for all residents in all aspects of our residency.

Finally, I wish to thank the US Navy for the opportunity to study Cariology and Operative Dentistry at IUSD and to Delta Dental for financially supporting this study.

TABLE OF CONTENTS

Introduction.....	1
Review of Literature.....	5
Methods and Materials.....	11
Results.....	19
Figures and Tables.....	23
Discussion.....	52
Summary and Conclusions.....	57
References	59
Abstract.....	65
Curriculum Vitae	

LIST OF ILLUSTRATIONS

FIGURE 1	A, B, show a polished monolithic low translucency LD, and a polished laminated high translucency LD veneer over low translucency LD substructure.....	24
FIGURE 2	Diagram showing the sample groups and the layers of each group.....	25
FIGURE 3	Lathe-cut 32-mm e.max CAD blocks.....	26
FIGURE 4	Bueller Isomet diamond saw.....	27
FIGURE 5	Leco polisher used to polish specimens to 1200 grit.....	28
FIGURE 6	Programat CS oven.....	29
FIGURE 7	E.max CAD Crystall/Connect.....	30
FIGURE 8	Whip-Mix vibrator.....	31
FIGURE 9	Prime and Etch, and Multilink resin cement.....	32
FIGURE 10	BluePhase curing light and Cure Rite curing light meter.....	33
FIGURE 11	Twelve-millimeter (12 mm) stainless steel push mold, e.max Ceram Build-Up Liquid.....	34
FIGURE 12	Instron E3000.....	35
FIGURE 13	Piston and 3 ball device with sample.....	36
FIGURE 14	Piston and 3 ball device with fractured sample.....	37
FIGURE 15	JEOL JSM-6390LV scanning electron microscope.....	38
FIGURE 16	Desk V, Denton Vacuum sputter coat machine.....	39
FIGURE 17	Gold Sputter coated specimens for SEM.....	40
FIGURE 18	Survival probability (Kaplan-Meier).....	41
FIGURE 19	Survival probability (Weibull model).....	42
FIGURE 20	Distribution of biaxial flexural stress.....	43
FIGURE 21	Scanning electron microscope images from each sample.....	47

TABLE I	Table of the materials and brands used to fabricate the specimens.....	48
TABLE II	Paired comparison results and p-values from Weibull reliability analysis.....	49
TABLE III	Weibull characteristic strength and modulus.....	50
TABLE IV	Biaxial flexural stress (MPa).....	50
TABLE V	Shows the biaxial flexural stress (MPa) on each layer of the material at a certain load (N).....	51

INTRODUCTION

One of the more popular esthetic all-ceramic restorative materials is lithium disilicate (LD). LD is available in two forms: (1) as an ingot, for use in a traditional lost wax processing technique (IPS e.max Press, Ivoclar Vivadent, Schaan, Liechtenstein); and (2) as a block that can be milled using computer aided design/computer aided manufacturing (CAD/CAM) technology (IPS e.max CAD, Ivoclar Vivadent, Schaan, Liechtenstein).¹ LD has a flexural strength of 396 MPa compared to 125 MPa for fine particle feldspar ceramic using a 3-point bend test.² The modulus of elasticity is favorable for LD (95 GPa) as it has been shown to be comparable to enamel (94 GPa).³ In addition, the coefficient of thermal expansion and the fracture toughness values for LD are similar to dentin.³ However, the hardness of LD (5.8 GPa) is higher than enamel (3.2 GPa).³ This has created some concern about possible wear of opposing dentition, but research has shown that a properly polished LD has the same occlusal wear rate as enamel.⁴ This increased strength comes from the 70-percent crystalline LD filler, and the fact that this material can be processed under pressure (“blue block” for CAD or the press process) to create a more uniform crystalline structure and also have fewer defects.⁵ Another major advantage of LD is that the glass matrix can be selectively removed with hydrofluoric acid to leave an etched surface to which silane can be applied to achieve excellent chemical bond strength when paired with a resin cement system.^{6,7} In addition, multiple shades and translucencies are available, offering practitioners a choice between a monolithic restoration or one that is reduced (“cut back”) and veneered with feldspathic porcelain (FP) to maximize esthetics.¹

Modern practice philosophy is to be as conservative as possible, preserving sound tooth structure and vitality of the dental pulp. The ability to bond for retention rather than solely relying on mechanical retention has allowed for less tooth structure reduction.⁸ Newer technology and material improvements led the manufacturer to recommend recently supported in-office or laboratory fabrication of thin (0.4-mm to 0.5-mm thick) LD CAD/CAM veneers.⁹ The use of a higher translucency LD veneer over a lower translucency LD crown substructure may result in a crown that has regained some of the more esthetic translucency and may reduce the occurrence of chipping seen with weaker traditional feldspathic veneers. Some evidence suggests that CAD/CAM fabricated LD veneering material on a substructure may be stronger than using traditional feldspathic veneering material.^{10,11} These restorations can be fabricated and delivered in a single clinical visit.¹² First, a lower translucency substructure is fabricated with a digitally created cutback, then a thin 0.5-mm high translucency LD veneer is fabricated and adhered/sintered to the substructure. Sintering of a LD veneer to a more opaque substructure (traditionally zirconia) is known as the CAD-On technique and it has shown promising results.¹⁰ This may improve esthetics and the overall speed of fabrication, and may possibly reduce fracture compared to veneering with feldspathic porcelain.

All-ceramic restorations tend to be fragile when placed in tension. They are especially vulnerable to defects and microcracks, which can develop during the processing steps. To evaluate all-ceramic restoration materials for use in the oral cavity, it is necessary to assess their resistance to fracture under load.¹³ Several performance tests can be used to assess the strength of ceramics. The biaxial flexure stress test (BFS) which can include ball on ring, ring on ring, and piston on three ball tests is one of them. An

advantage to this type of test over a three-point flexural test is that it is less sensitive to flaws and defects near the edges of the specimens.^{13,14} Using a test that is not sensitive to the edges of the specimens leads to results that are typically considered more reliable.¹⁴ It is necessary to evaluate whether using a CAD/CAM fabricated LD veneer over a LD substructure would increase the strength of the restoration above what we see with using a FP veneer on a LD substructure. The purpose of this project was to investigate the effect of using different LD veneer application methods to a LD substructure on the fatigue resistance of LD veneer/substructure restorations. The null hypothesis was that adhering or sintering a thin laminate layer of LD on another LD substructure will not result in increased fatigue resistance in comparison to sintered FP on LD.

REVIEW OF LITERATURE

LITHIUM DISILICATE

Dental ceramic restorations have become particularly appealing due to their esthetics, durability, and biocompatibility.⁶ A very popular dental ceramic is LD, which has been studied since 1959, it was recognized that by controlling the crystallization and nucleation of glasses, using variations in temperature and time held at a certain temperature, can result in a product with improved mechanical properties.¹⁵ LD based dental ceramics have become popular because they have improved durability and strength beyond conventional dental porcelains.⁶ This increased strength comes from the 70-percent crystalline LD filler, and this material can be processed under pressure to create a more uniform crystalline structure and also have fewer defects.⁵ Another major advantage of LD is that, as a glass ceramic the glass matrix can be selectively removed with hydrofluoric acid to leave an etched surface to which silane can be applied to achieve excellent chemical bond strength when paired with a resin cement system.^{6,7} Because of its high strength, lithium disilicate is often used as a rigid core to which a more esthetic layer of material is added. Traditionally this has been feldspathic porcelain, which has inferior mechanical properties.¹⁶

In 2006 the use of LD in a chairside CAD/CAM mill was made possible because of a two-stage crystallization process.⁵ The first stage precipitates 40-percent lithium metasilicate crystals which creates a blue/violet color block formation with a crystal size of 0.2-1.0 μm .⁵ This step is essential to being able to mill the material in a milling unit because it is softer, and therefore less damage occurs to the material and to the diamond burs in the mill, compared to the harder LD. After milling in this “blue block” phase the

ceramic can then be crystallized at 850° C while under vacuum for 20 minutes to 25 minutes to become LD. The final grain size is 1.5 µm and it is 70-percent volume of LD crystals in a glassy matrix.^{1,5} It is, however, necessary to return the surface to a high polish or glaze as non-polished surface prepared by diamond burs, like those used for the CAD process, have been shown to negatively influence fracture resistance.¹⁷

COMPUTER-AIDED DESIGN/COMPUTER-AIDED MANUFACTURING (CAD/CAM)

The initiation of CAD/CAM in dentistry started in an effort to move away from having analog models that involve a lot of steps. The lost wax technique involves the need to control or compensate for the small changes in expansion and contraction that take place in the process of fabricating an indirect restoration. Between impression materials, stone models, waxed restorations, investing, and casting there are many opportunities for error to be introduced. CAD/CAM technologies were introduced to the dental community in 1971.¹⁸ However, it was not until a conference in 1983 that the first crown was milled and delivered on a patient.¹⁸ Recently, utilization of CAD/CAM technology to fabricate ceramic dental restorations has become common.^{1,5,19}

CAD/CAM offers the speed and reproducibility of digital technology and lessens the dependence on the manual skills of the laboratory technician. However, the monolithic composition of many CAD/CAM ceramic blocks limits the esthetic appearance of CAD/CAM-fabricated restorations. Overlaying a more translucent and esthetically appealing, placed by hand, sintered porcelain onto the stronger ceramic substructure improves esthetics, while maintaining good strength.^{20,21}

PORCELAIN CHIPPING

According to a 10-year study, Tiechmann et al. found that a major challenge with feldspathic veneered LD substrate crowns was chipping of the veneering material.²² At five years, the annual chipping rate was 3.08 percent; however, the rate dropped to a more acceptable 1.5 percent at the ten-year follow-up. The authors decided that the early chipping was most likely not due to fatigue phenomenon, but, rather, to errors that were made during the manufacturing process.²² Decreased fracture loads were also demonstrated in a study by Zhao et al. in which fracture loads were significantly lower for feldspathic veneered LD specimens in comparison to monolithic LD specimens.²³ This is a challenge with using feldspathic porcelain placed by hand, in that it can be susceptible to errors during its application, and this may lead to an increased failure rate for the restoration. Jian et al. confirmed that there were more defects in the feldspathic veneering layer than in the monolithic layers.²⁴ This knowledge guides the desire to find a mechanically stronger veneering material that is more resistant to fracture and chipping.¹⁰

Wattanasirmkit investigated ways of improving the shear bond strength of feldspathic porcelain on zirconia substructures by adding a liner of LD in between the two.²⁵ A layer of LD glass ceramic paste was applied onto a sintered zirconia substructure and fired before adding multiple layers of feldspathic porcelain. Specimens with the LD liner had a statistically significant increase in shear bond strength compared to the specimens where feldspathic porcelain was added directly to the zirconia substructure.²⁵

LAMINATION

The process of adhering a layer of one material to another material using a resin composite luting agent is known as lamination and has been used in other industries to increase flexural strength and interrupt crack propagation.²⁶ This process has demonstrated an increase in flexural strength for crowns using dental zirconia as the crown substructures laminated with a resin-bonded feldspathic veneers.²⁶ However, we found no reports in the literature using the same process with LD materials as the crown substructure and veneer. This lamination technique could potentially allow improved esthetics while maintaining very good strength in comparison to monolithic restorations.²⁶

STEPWISE STRESS BIAXIAL FLEXURE TESTING

Dental ceramics are a brittle material and prone to fracture.²⁷ Typically, dental restorations do not fail due to extreme loads, but rather clinically they fail due to cyclic fatiguing of the material.²⁸ For this reason a popular method for assessing the fatiguing of dental ceramics is to use a stepwise stress testing method, in which a non-static load is gradually increased.²⁹ Stepwise stress testing can be carried out using a number of methods. One popular method is to use a biaxial flexure test, in which a load is applied through a single contact on top of the specimen while it is supported underneath by multiple points in the shape of a ring.²⁹

SUMMARY OF THE REVIEW OF THE LITERATURE

Testing and clinical use of LD as a veneering material on a zirconia substructure has been documented.³⁰ Also, there has been limited research in using LD that has been

placed by hand in a manner similar to how feldspathic porcelain has been used.¹⁰ The use of digitally created CAD/CAM veneers on a single tooth restoration has been documented, but not with LD veneering materials.¹¹ Lamination has been used as a way to improve esthetics by varying translucencies, and possibly shades, to create more natural esthetics compared to a monolithic restoration.³ External staining of a monolithic restoration is currently used, but this has some limitations due to the difficulty of using colored pigments to mimic translucency and there are some concerns about the longevity of external stains.³¹ Currently there is no published research that has studied using a LD veneer over a LD substructure and the effects of laminating these materials for use as a dental prosthesis. The question this article addresses is whether or not there is a potential to return to similar fracture resistance of monolithic LD compared to bilayer LD. This could potentially help to guide the next step in esthetic dental restorations that use a high strength ceramic as a veneering layer while using the same high strength material as a substructure, both of which can be fabricated quickly using a CAD/CAM chairside system. This type of restoration could also potentially help to move from a reliance on chairside external staining or dental laboratories to create appropriately translucent all-ceramic restorations.

MATERIALS AND METHODS

SPECIMEN FABRICATION

This was a laboratory study. No human subjects were used. The flexural strength of LD veneering materials sintered or bonded to LD, and FP sintered to LD were compared to that of monolithic LD utilizing ceramic discs ($\text{Ø}=12 \times 1.2 \text{ mm}$) ($n = 15$). Specimen fabrication and testing conformed to ISO/FDIS 6872:2014(E).

Four different disc shaped sample groups were fabricated to have a final dimension of 12-mm diameter with a total thickness of 1.2 mm (Figure 2; Table 1). Non-crystallized LD blocks (e.max CAD, Ivoclar Vivadent, Shaan, Liechtenstein; Lot# W93529; Figure 3), 32 mm in length, were machined into cylinders on a lathe to create uniform, round 12-mm diameter cylinders. Then, each cylinder was sectioned using a low speed diamond saw (Isomet 1000, Buehler, Lake Bluff, Illinois, USA; Figure 4). To obtain a uniform and flat surface, finishing and polishing steps (Leco DS-20, Saint Joseph, Michigan, USA) were performed under running water using #600, #800, & #1,200-grit silicon carbide paper.²⁶ For the three experimental groups (SLDV, RBLDV and SFV), “crown substructure” discs fabricated from LD cylinders ($\text{Ø} = 12 \times 32 \text{ mm}$) were sectioned into 0.8-mm thick discs, polished and then crystallized in a furnace (Programat CS Furnace, Ivoclar Vivadent, Shaan, Liechtenstein; Table 2). There were no more than five specimens fired at a time during a firing cycle. Final thickness of each substructure specimen after polishing was 0.7 mm. Specimens were stored in a constant temperature oven at 22°C.

EXPERIMENTAL GROUPS

Monolithic LD, MLD

The control group consisted of monolithic LD specimens (MLD) 1.3 mm in thickness. The final thickness of each specimen after polishing (Figure 5) was verified with a micrometer to be 1.2 ± 0.05 mm. After polishing, the LD specimens were crystallized at the prescribed firing cycle following the manufacturer's guidelines (Figure 6).

THIN LD VENEER SINTERED TO LD SUBSTRUCTURE, SLDV

Thin veneers ($\varnothing=12\times 0.5$ mm) of pre-crystallized 32-mm LD were cut, polished and crystallized using the same methods described above. The 0.5-mm thickness is the minimum thickness recommended by the material manufacturer for CAD/CAM thin veneers (E.max IPS CAD). To create this specimen group a 0.5-mm veneer disc was sintered it to a 0.7-mm LD substructure disc. A thin layer of connecting porcelain (IPS e.max CAD Crystall/Connect, Ivoclar Vivadent, Shaan, Liechtenstein; Lot# W01285; Figure 7) was placed on the thicker LD sample and then the thin LD disc was positioned on top. A thin 0.05-mm sheet of acetate film was placed above and below the specimens to create uniformity of pressure distribution with a 200 g weight applied for 1 minute, while vibrating (Heavy Duty Vibrator, WhipMix, Louisville, KY, USA; Figure 8). Excess connecting porcelain was removed by a plastic instrument and brush while still under pressure. The specimens were then fired (no more than 5 specimens at a time) at the manufacturer's recommended temperature (Table 2). To account for the thickness of the connecting sintering porcelain the specimens were re-sized (returned to 1.2 mm at the

expense of the 0.7-mm substructure disc), and re-polished up to 1200 grit in the same manner as previously described. The specimens were remeasured to assure they had returned to the previously allowed dimensions of 1.2 ± 0.05 mm

THIN LD VENEER RESIN-BONDED LD SUBSTRUCTURE, RBLDV

A thin LD veneer ($\varnothing = 12 \times 0.5$ mm) was resin bonded to the surface of a LD substructure ($\varnothing = 12 \times 0.7$ mm), creating an overall final specimen thickness of 1.2 mm. A single surface of each specimen was prepared for bonding using a self-etching primer (Ivoclar Monobond Prime and Etch, Ivoclar, Vivadent, Shaan, Liechtenstein; Lot # X46577; Figure 9) that was actively applied with a microbrush for 20 seconds, allowed to sit for 40 seconds, and thoroughly rinsed under running water for 30 seconds (according to manufacturer instructions). A small amount of resin cement (transparent) was placed on the center of the substructure disc (Multilink, Ivoclar Vivadent, Shaan, Liechtenstein; Lot# X21834; Figure 9). The veneer was lightly positioned onto the prepared surface of the substructure disc. An acetate film was applied above and below the discs for uniformity of dispersion of forces. A 200 g weight was applied on top for 30 seconds for consistent pressure between specimens.³² The specimens were tack cured for 2 seconds around the periphery, excess resin was removed with a plastic instrument, and light cured (Bluephase Light, Ivoclar Vivadent, Shaan, Liechtenstein; Figure #10) for 2 minutes at 6 different locations (3 locations approximately 120° apart on veneer side of the specimen and then the same on the substructure side) on the disc for 20 seconds each. A visible curing light meter was used at the beginning of each bonding session to assess the light intensity generated by the light curing unit (Cure Rite, DENTSPLY Sirona, York, PA, USA; Figure #10). Outputs were recorded between 1150-1250 mW/cm². Due to the low

thickness of the resin cement, there was no need to refinish the discs to obtain a 1.2-mm thick sample. The RBLDV specimens were stored dry in the constant temperature oven at 22°C, until the resin bonding, then they were stored in water for 24 hours prior to testing.

FELDSPATHIC VENEER SINTERED ONTO LD SUBSTRUCTURE, SFV

Feldspathic porcelain was sintered on the surface of 0.7-mm LD specimens to simulate a traditional veneer-ceramic condensation process. These specimens were prepared by placing each selected LD disc into a stainless-steel mold ($\text{Ø} = 12 \times 1.3$ mm) (Figure 11). Following manufacturer instructions, a thin wash layer slurry of feldspathic veneering ceramic (e.max Ceram, Ivoclar Vivadent, Shaan, Liechtenstein; Lot# W89584; Figure 10) was combined with a build-up liquid (e.max Ceram build up liquid, Ivoclar Vivadent, Shaan, Liechtenstein), this slurry was placed onto the 0.7-mm disc, and then vibrated to remove any air bubbles. The excess liquid was absorbed with an absorbent tissue paper. Specimens were then vacuum-fired and allowed to cool to room temperature. A second layer was placed and fired using the same protocol.³² If necessary, a third firing cycle was used to complete the specimens. To accommodate for any shrinkage of the veneering porcelain, the specimens were purposefully thickened by an additional 0.1 mm. For these specimens, finishing and polishing was performed, on the feldspathic veneer side, using the same protocol as previously listed to obtain a polished, uniform 1.2-mm thickness of the entire specimen.

STEPWISE STRESS TESTING USING BIAXIAL FLEXURAL STRESS TEST

Testing was performed dry with biaxial flexure test using a piston-on-ring configuration following ISO/FDIS 6872:2014(E). The fabricated specimens were tested

up to 215,000 cycles at room temperature (22°C) using a stepwise stress fatigue test. The specimens were conditioned at 50 N for 5,000 cycles; then the applied load was increased by 50 N increments every 30,000 cycles with a load ranging from 100 N up to 400 N. A frequency of 1.4 Hz on a universal testing machine (Electropuls E3000, Instron, Norwood, MA, USA; Figure #12) was used with a cross-head speed of 0.5 mm/min until fracture occurred. The load was applied using three hardened steel balls with 4.5 mm diameter (radius 2.25 mm) placed 120 degrees apart on a support circle with a diameter of 11 mm (radius 5.5 mm). Load was applied with a flat piston with a diameter 1.4 mm (radius 0.7 mm) at the center of the specimen (Figure 13 and 14). To evenly distribute the forces, a 0.05-mm thick acetate film was placed above and below the specimen.^{13,27} Each specimen was checked for cracks and/or failures every 30,000 cycles under a light microscope.³³

The Poisson's ratios and Young's modulus for the materials used were: e.max CAD 0.20, 95 GPa; Multilink 0.28, 18.6 GPa; Fusion Ceramic 0.21, 70 GPa; e.max Ceram 0.23, 90 GPa respectively.^{34,35} The variation of the stresses through the thickness for the bilayer discs was calculated according with the equations 1 and 2 proposed by Hsueh et al. varying the thickness from 0.1 mm to 1.2 mm.³⁶

$$\sigma_{r1} = \sigma_{\theta1} = \frac{-PE_1(1+\nu)(Z-Z_n^*)}{8\pi(1-\nu_1^2)D^*} \times \left[1 + 2 \ln\left(\frac{a}{c}\right) + \frac{1-\nu}{1+\nu} \left(1 - \frac{c^2}{2a^2} \right) \frac{a^2}{R^2} \right] \quad (1)$$

(for $0 \leq Z \leq t_1$ and $r \leq c$),

$$\sigma_{r2} = \sigma_{\theta2} = \frac{-PE_2(1+\nu)(Z-Z_n^*)}{8\pi(1-\nu_2^2)D^*} \times \left[1 + 2 \ln\left(\frac{a}{c}\right) + \frac{1-\nu}{1+\nu} \left(1 - \frac{c^2}{2a^2} \right) \frac{a^2}{R^2} \right] \quad (2)$$

(for $t_1 \leq Z \leq t_1 + t_2$ and $r = c$),

Where a , c and R are the radii of the supporting ring, piston and disc, respectively and considering r the radial distance from the center of the disc and r , θ and Z cylindrical coordinates. The neutral surface position and the flexural rigidity for all bilayer groups were obtained from the equation 3 and 4, respectively.

$$Z_n^* = \frac{\frac{E_1 t_1^2}{2(1-\nu_1^2)} + \frac{E_2 t_2^2}{2(1-\nu_2^2)} + \frac{E_2 t_1 t_2}{1-\nu}}{\frac{E_1 t_1}{1-\nu_1^2} + \frac{E_2 t_2}{1-\nu_2^2}} \quad (3)$$

$$D^* = \frac{E_1 t_1^3}{3(1-\nu_1^2)} + \frac{E_2 t_2^3}{3(1-\nu_2^2)} + \frac{E_2 t_1 t_2 (t_1 + t_2)}{1-\nu^2} - \frac{\left[\frac{E_1 t_1^2}{2(1-\nu_1^2)} + \frac{E_2 t_2^2}{2(1-\nu_2^2)} + \frac{E_2 t_1 t_2}{1-\nu^2} \right]^2}{\frac{E_1 t_1}{1-\nu_1^2} + \frac{E_2 t_2}{1-\nu_2^2}} \quad (4)$$

Where E is the Young's modulus of each ceramic, t_1 and t_2 is the overall thickness of each layer and the Poisson's ratio of the bilayered disc calculated by the equation 5.

$$\nu = \frac{\nu_1 t_1 + \nu_2 t_2}{t_1 + t_2} \quad (5)$$

For the monolithic discs the stress variation was calculated through equation 6 and 7.³⁶

$$\sigma_r = \sigma_\theta = \frac{3P(1+\nu)}{4\pi h_n^3} \times \left[1 + 2 \ln \left(\frac{a}{c} \right) + \frac{1-\nu}{1+\nu} \left(1 - \frac{c^2}{2a^2} \right) \frac{a^2}{R^2} \right] \quad (6)$$

(at $z=0$ and $r \leq c$),

$$\sigma_r = \sigma_\theta = \frac{-3P(1+\nu)(z - \frac{h_n}{2})}{2\pi h_n^3} \times \left[1 + 2 \ln \left(\frac{a}{c} \right) + \frac{1-\nu}{1+\nu} \left(1 - \frac{c^2}{2a^2} \right) \frac{a^2}{R^2} \right] \quad (7)$$

SCANNING ELECTRON MICROSCOPY

Specimen fragments that fractured during the stepwise stress testing were viewed in a scanning electron microscope (JSM-6390LV, JEOL, Peabody, MA, USA; Figure #15) was performed. Specimens were placed on aluminum stubs with carbon adhesive tabs, (Electron Microscopy Sciences, Hatfield, PA) and a gold-palladium thin layer was coated for 120 seconds, (Denton Vacuum, Moorestown, NJ). Digital images were obtained and submitted to qualitative evaluation to provide insight regarding the stresses caused on the specimens at the fracture time, and also the sequence of events that lead to the fracture. Specimens representing the highest and lowest strength from each group were selected for imaging.³²

SAMPLE SIZE

With a sample size of 15 specimens per group, the study had 80-percent power to detect a 25-percent difference in biaxial flexural stress between any two groups, assuming two-sided tests conducted at a 5-percent significance level.^{12,26}

RESULTS

The biaxial fatigue resistance mean, standard deviation, Weibull characteristic strength, and Weibull modulus were summarized for each group. Weibull parametric survival analysis was used to compare biaxial flexural fatigue resistance among the four groups. A 5.0-percent significance level was used for each test.

A Weibull-distribution survival analysis compared the differences in fatigue resistance among the four groups. The fatigue resistance (Newtons) was used as time to event for the analysis. The Weibull characteristic strength (Table 3) was found to be 314.5 for RBLDV, 256.8 for SFV, 289.7 for MLD, and 305.2 for the SLDV groups. The results (Table 4), show that both the RBLDV and SLDV ($p = 0.0174$, and $p = 0.036$ respectively) had a statistically significantly greater fatigue resistance than the SFV group. The fatigue resistance to fracture between the two LD veneer groups compared to the MLD group was not statistically significant ($p = 0.26$ for RBLDV to MLD, and $p = 0.49$ for SLDV to MLD). The difference between the MLD and SFV groups was also not statistically significant ($p = 0.17$). In addition, the Weibull modulus was found to be 4.6 for MLD, 5.6 for SLDV, 6.2 for RBLDV, and 4.1 for SFV groups. The survival probability was shown using both a Kaplan Meier, and Weibull model for the various materials (Figure 18 and 19).

A non-parametric test was used to compare the number of pieces created upon fracture between the groups. The increased number of pieces the RBLDV broke into was statistically significant, when compared to other sample groups ($p=0.0008$ MLD, <0.0001 SLDV, and 0.0002 SFV). In addition, the total number of cycles were compared using a

one-way ANOVA with factor for group to identify the differences between the groups. The results were not statistically significant ($p=0.06$).

Stress testing determined where the compressive and tensile forces were concentrated in the sample at a certain load (Table 5). The biaxial flexural stress results are presented (Figure 20 A-D) for each sample group at the outer surface of each layer. $Z=0$ represents the bottom of the thicker LD substructure, and the $z=1.2$ or 1.05 represents the upper surfaces of the veneer layers. The positive stress values to the right of zero represent the tensile forces while the negative stress values to the left of zero represent the compressive forces.

To observe if some specimens were more stable or that they presented less variance at the time of fracture, a homogeneity of variance test was conducted. This test looked at whether or not a group had a statistically significant greater range of when the specimens would break. Results showed a no statistically significant differences ($p=0.2735$).

Scanning electron microscope images were qualitatively evaluated for porosities or cracks (Figure 21 A-D). The MLD sample (figure 21A) shows a uniform surface with no porosities or voids, which is expected from a manufactured LD CAD material. Figure 21B shows a specimen from the SLDV group. Of interest were the stress lines noted at the base of the veneer sample radiating from the sintered connecting porcelain. These stress lines were not noted in the other groups. Also, there were occasional small voids within the connecting feldspathic porcelain material of the SLDV group. Additionally, the figure 21D (SFV group) shows the high number of porosities within the feldspathic porcelain. Each one of these imperfections can act to increase the stress within the

feldspathic veneer sample leading to a decrease of the material strength. The CAD materials were consistently more uniform, especially in comparison to the feldspathic material. Porosities were not found in the RBLDV group (figure 21C).

FIGURES AND TABLES



FIGURE 1. A) Polished low translucency LD substructure without veneering or staining. B) Polished higher translucency LD veneer was bonded to a lower translucency substructure to create a more realistic and esthetic restoration.

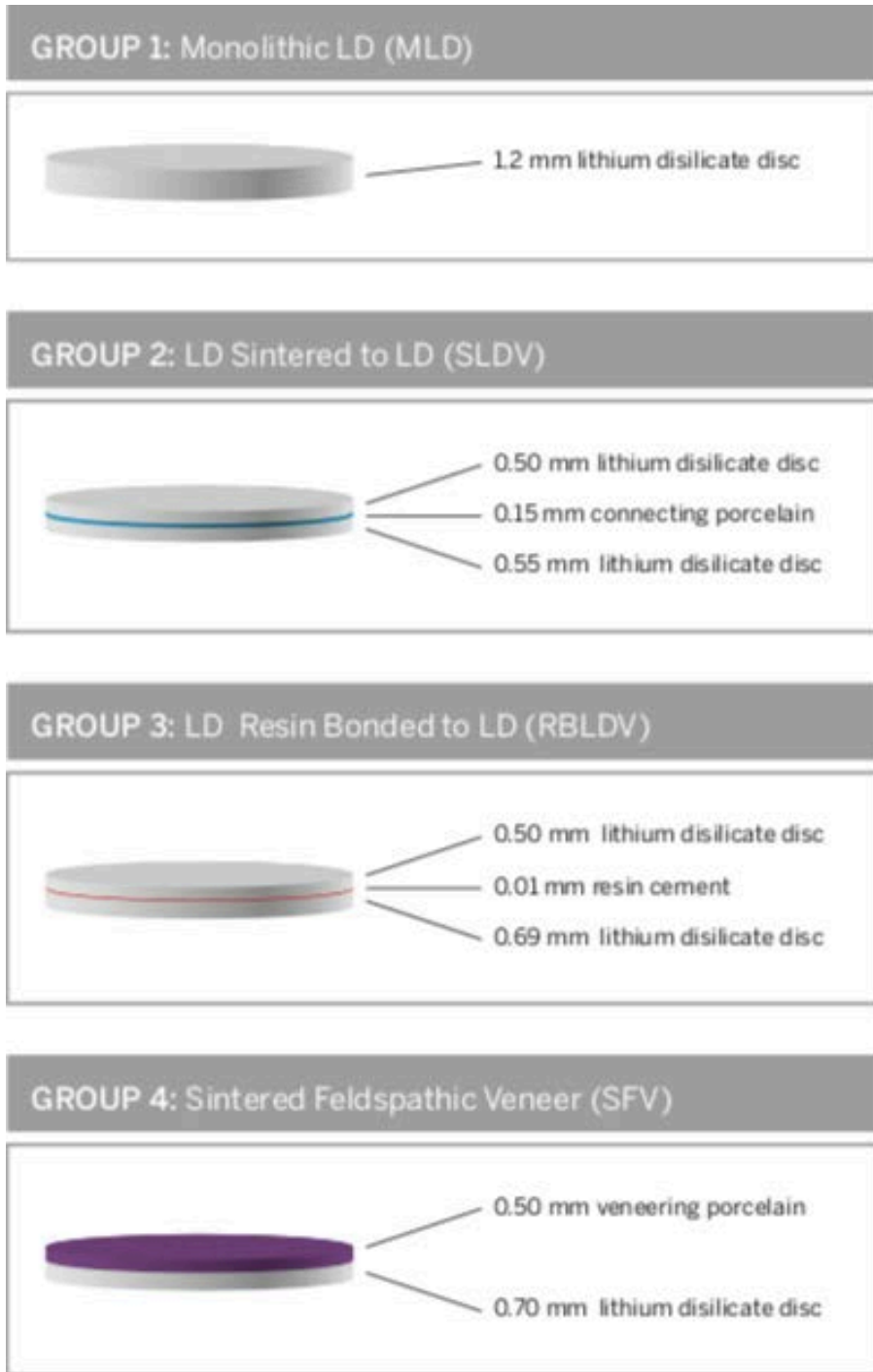


FIGURE 2. Showing the sample groups and the various layers of each sample group.



FIGURE 3. Lathe-cut (to create cylinder shape) 32-mm long e.max CAD block 12-mm wide for specimens ready to cut.

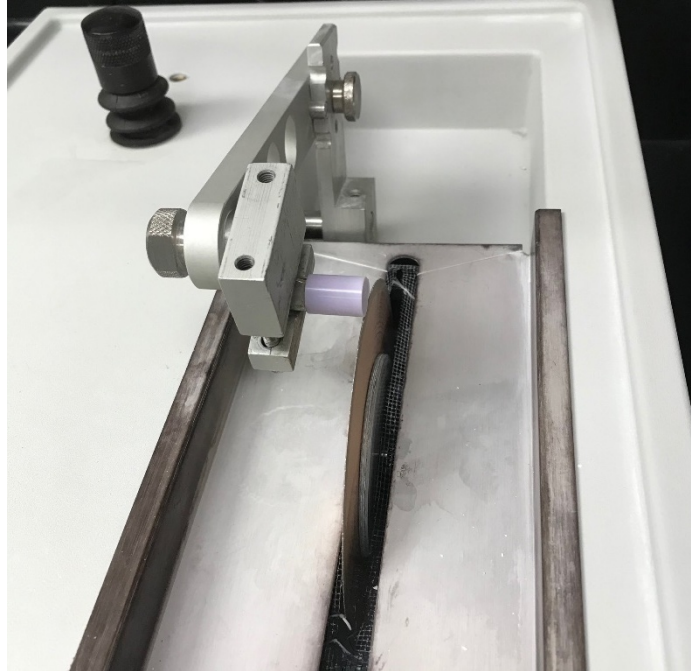


FIGURE 4. Shows the Bueller Isomet diamond saw preparing to cut a specimen.



FIGURE 5. Leco polisher used to polish specimens up to 1200- μm grit.

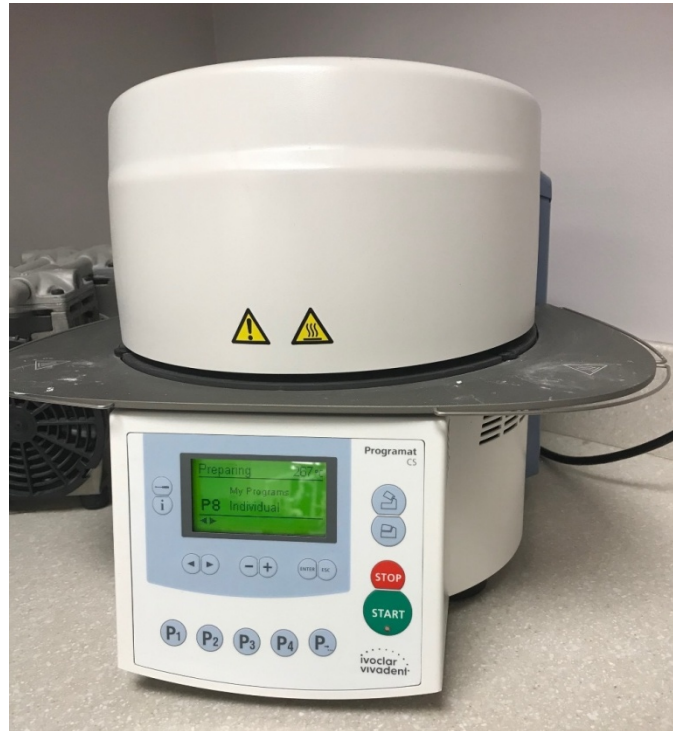


FIGURE 6. Shows the Programat CS oven.



FIGURE 7. Crystall./Connect.



FIGURE 8. Vibrator, Whip-Mix.



FIGURE 9. Prime and Etch (Left), Multilink Resin



FIGURE 10. BluePhase Curing Light (left), Cure Rite curing light meter (right).



FIGURE 11. Twelve-millimeter (12-mm) stainless steel push mold (left), e.max Ceram (center) and Build-Up Liquid (right).

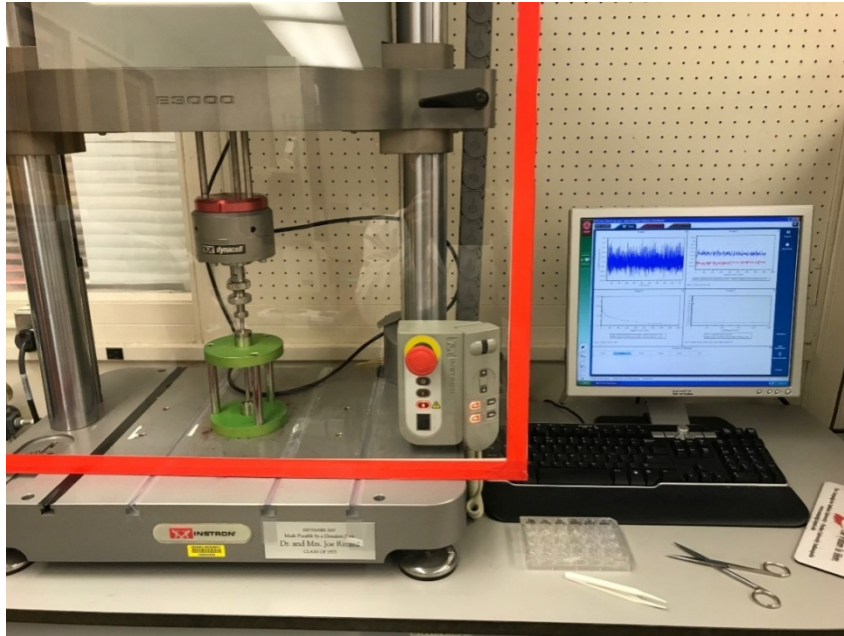


FIGURE 12. Demonstrating the Instron E3000 in use with specimen during.

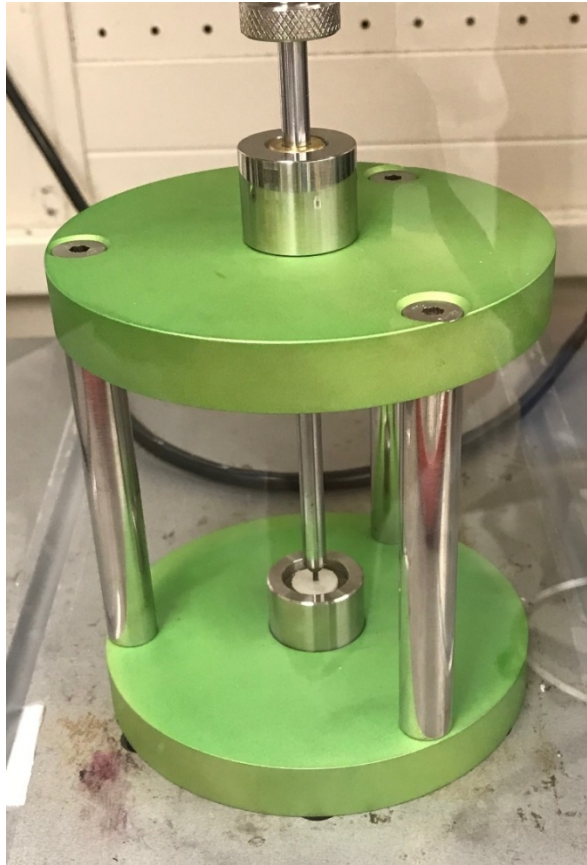


FIGURE 13. Demonstrating a specimen placed with protective films above and below it mounted on the piston and 3 ball device.

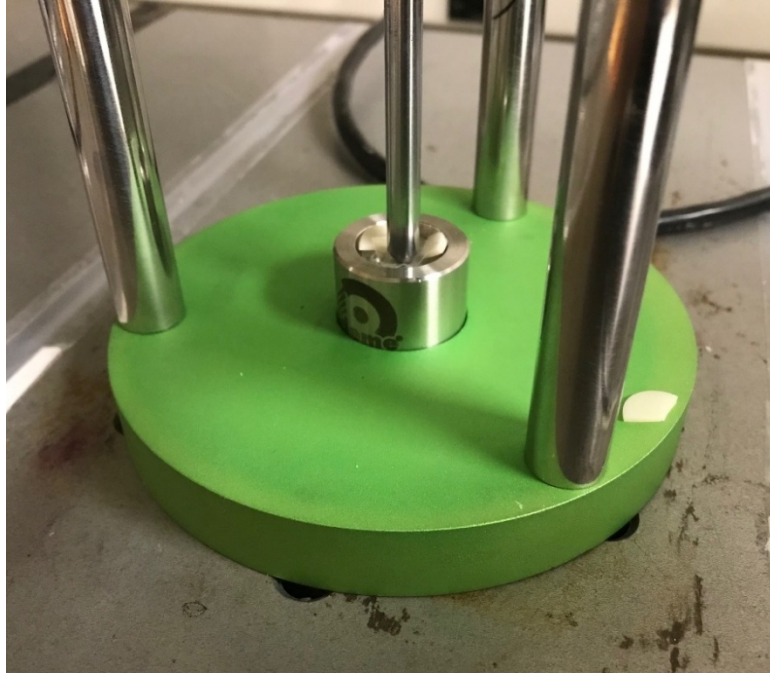


FIGURE 14. Shows a broken sample.



FIGURE 15. JEOL JSM-6390LV scanning electron microscope.



FIGURE 16. Desk V, Denton Vacuum sputter coat machine.



FIGURE 17. Gold sputter coated specimens ready for SEM imaging.

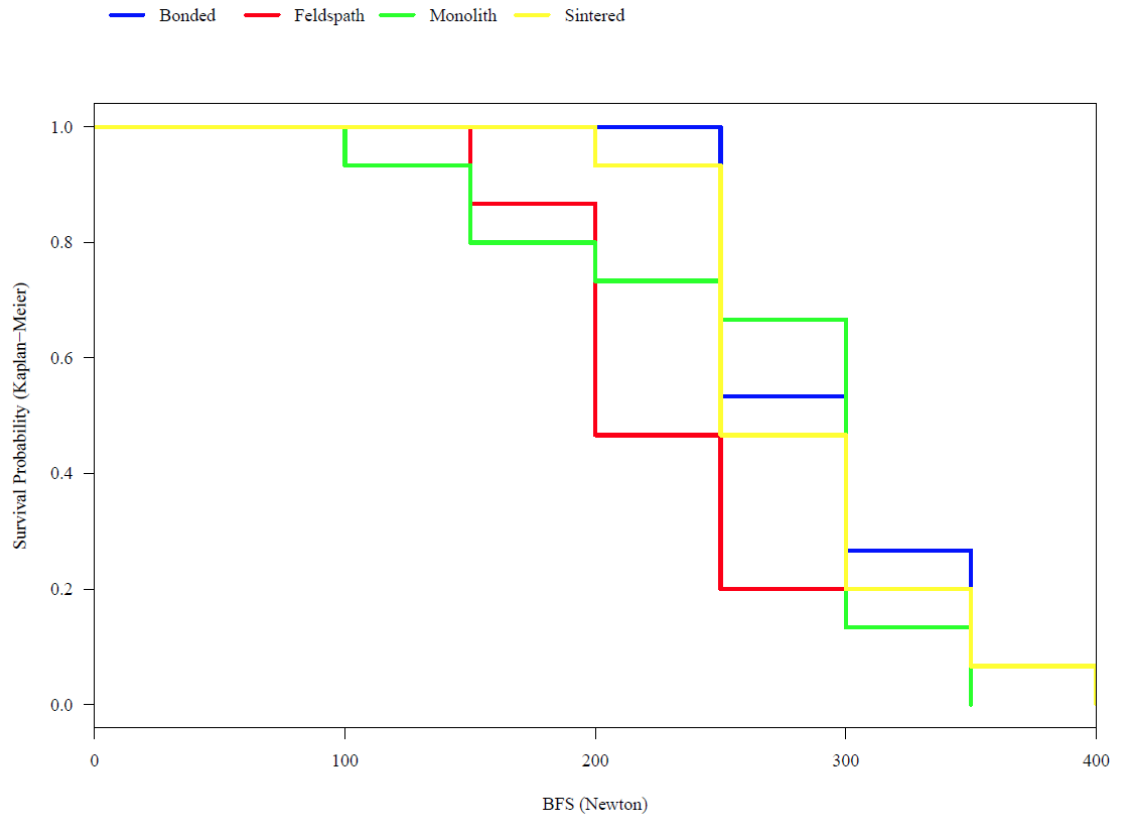


FIGURE 18. Survival probability (Kaplan-Meier).

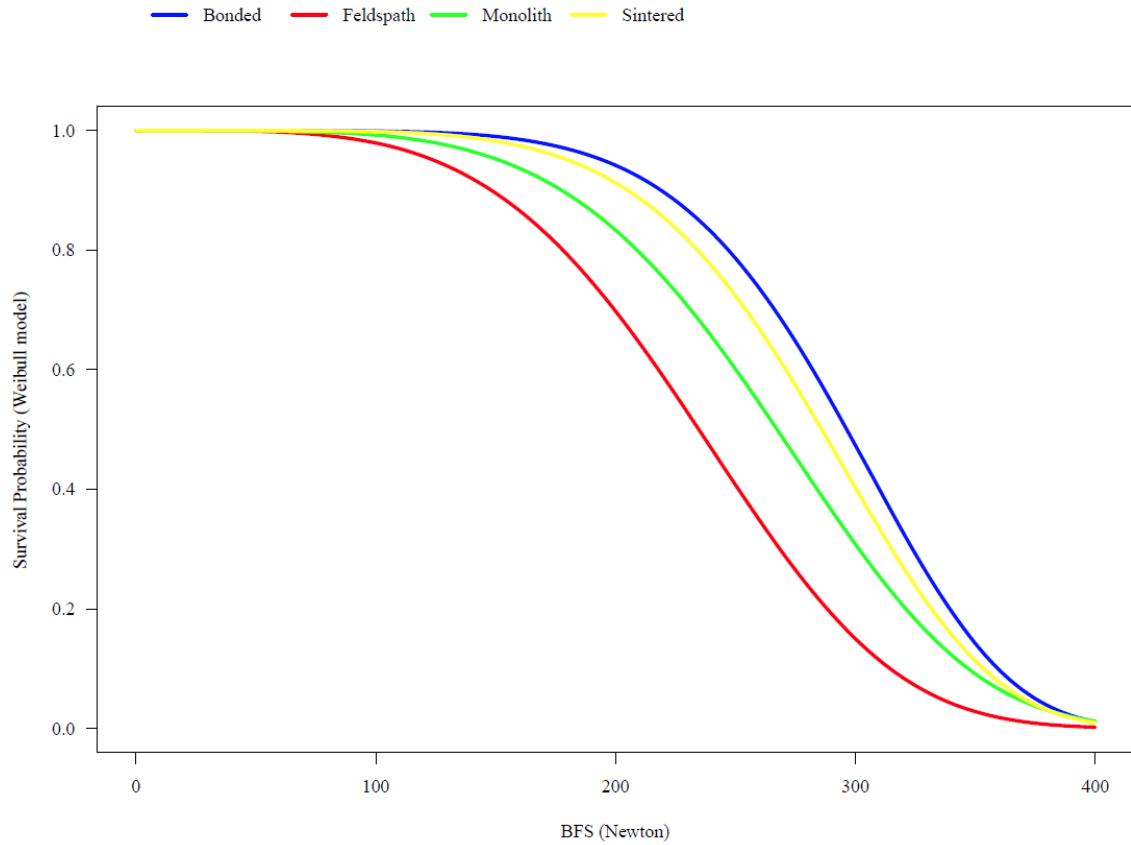


FIGURE 19. Survival Probability (Weibull model): Representing the probability of the specimens failing at a certain BFS (Newton) load.

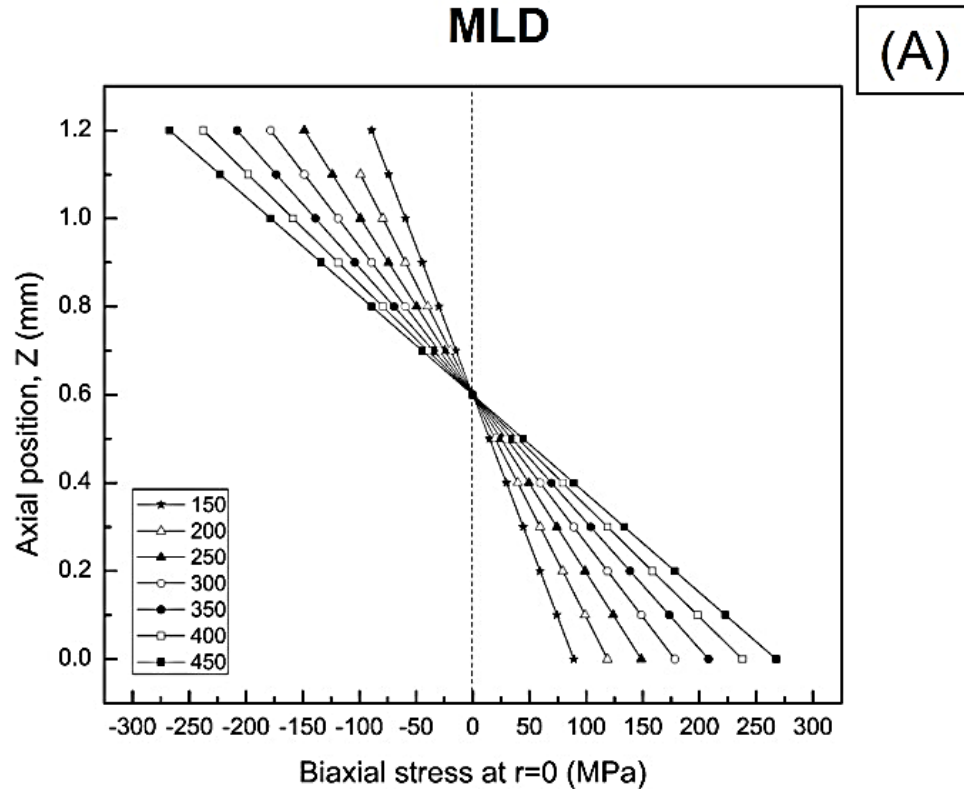


FIGURE 20. Shows the distribution of biaxial flexural stress on the specimens.
A = MLD.
(continued)

SLDV

(B)

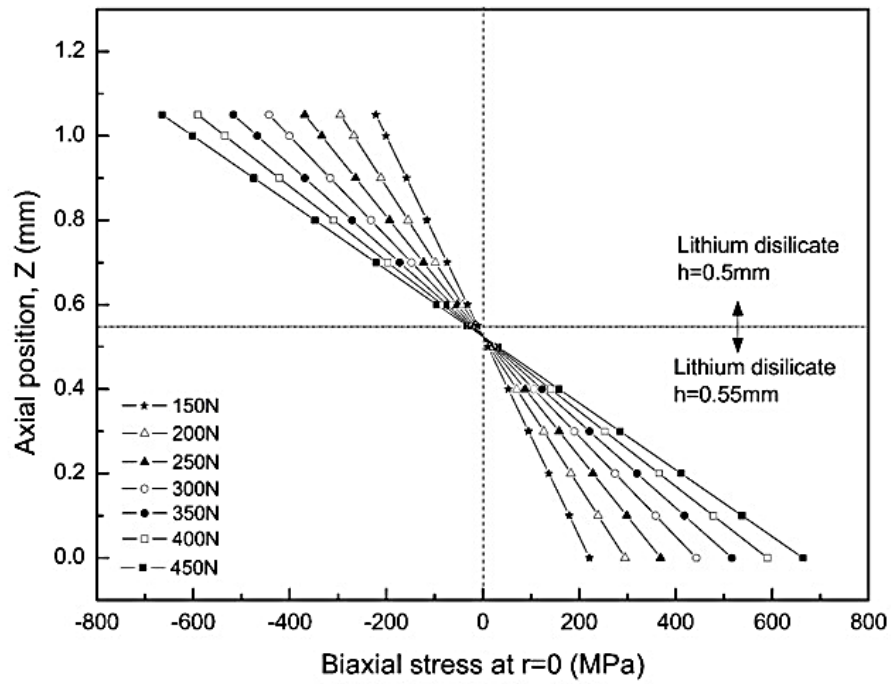


FIGURE 20 (cont.) Shows the distribution of biaxial flexural stress on the specimens.
 B = SLDV.
 (continued)

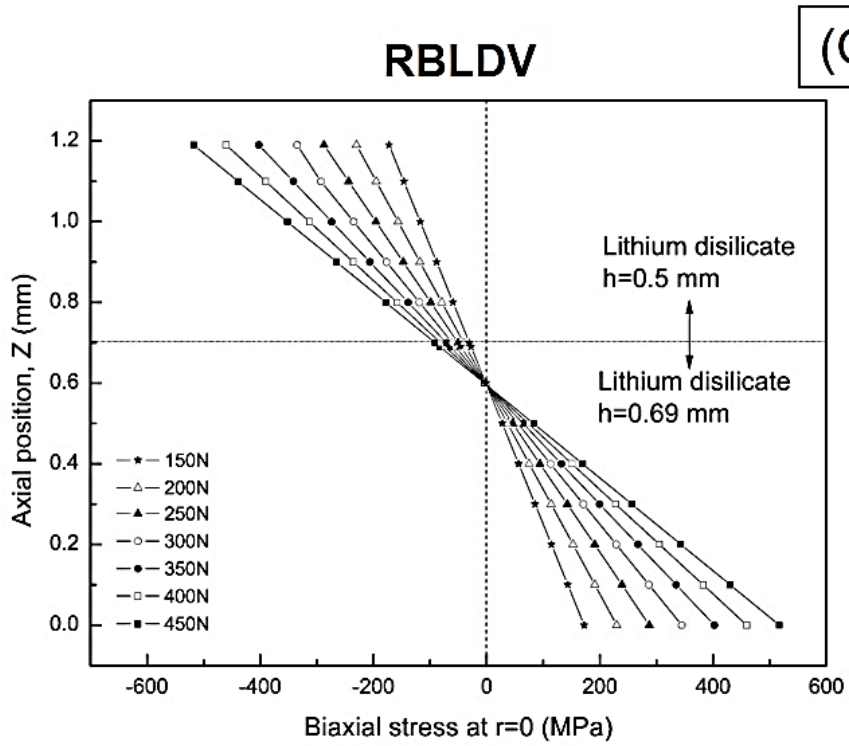


FIGURE 20 (cont.) Shows the distribution of biaxial flexural stress on the specimens. C = RBLDV. (continued)

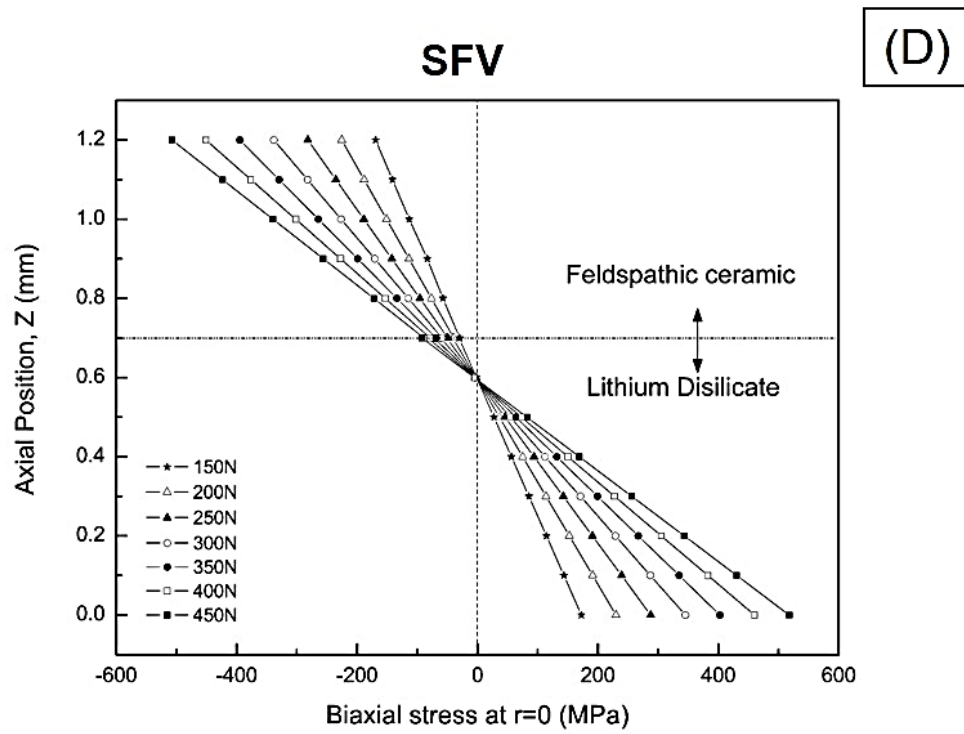


FIGURE 20 (cont.) Shows the distribution of biaxial flexural stress on the specimens.
D = SFV.

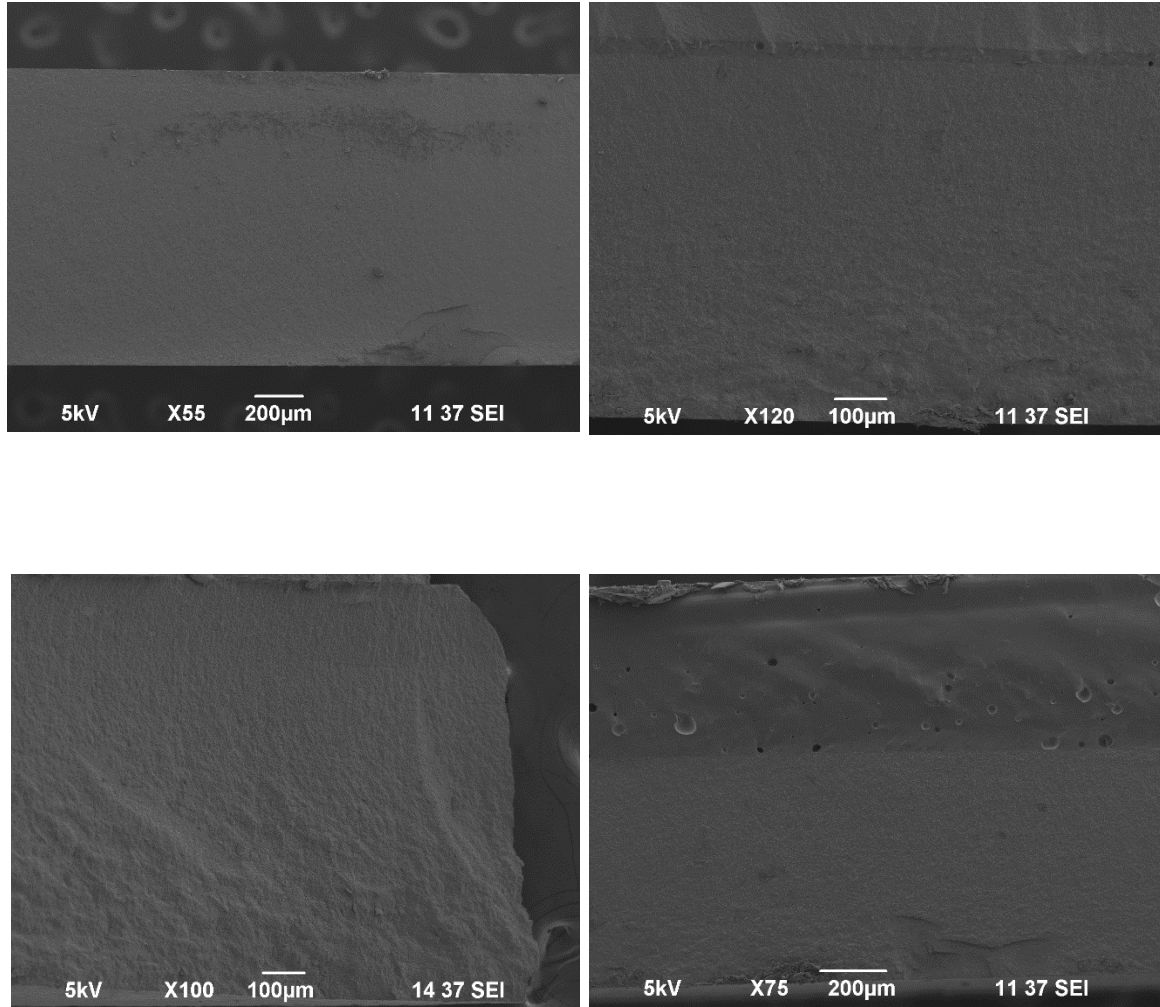


FIGURE 21. (A) MLD; (B) SLDV; (C) RBLDV; (D) SFV showing scanning electron microscope images of specimens.

TABLE I

Showing the groups and materials tested

GROUP	TECHNIQUE	MATERIALS
GROUP 1: (Control) (Lithium Disilicate) (MLD)	Monolithic lithium disilicate	e.max CAD, Ivoclar
GROUP 2: (Sintered Thin LD Veneer) (SLDV)	Thin lithium disilicate veneer sintered to lithium disilicate base	e.max CAD, Ivoclar; crystall./connect, Ivoclar
GROUP 3: (Resin Bonded Thin LD Veneer) (RBLDV)	Thin lithium disilicate veneer resin bonded to lithium disilicate base	e.max CAD, Ivoclar; multiink, Ivoclar
GROUP 4: (Sintered Feldspathic Porcelain Veneer) (SFV)	Veneering ceramic sintered onto lithium disilicate base	e.max CAD, Ivoclar; e.max ceram, Ivoclar

TABLE II

Programat cs firing table* used for the crystallization of LD, sintering of LD to LD (CAD-on), and placing the e.max Ceram wash, and then dentin layers**

		A	B	C	D	E	F	G
IPS e.max CAD	Crystall /Glaze	403	6:00	90/30	820/840	00:10/07:00	550/820	820/840
IPS e.max CAD-on	Fusion/ Crystall.	403	2:00	30/30	820/840	2:00/7:00	550/820	820/840
IPS e.max Press Layering Tech.	Wash firing (foundation) 1st/2nd	403	4:00	90/20	650/730	0:00/2:00	650/730	650/729
IPS e.max Press Layering Tech.	Dentin/ Incisal firing	403	4:00	90/20	650/730	0:00/2:00	650/730	650/729

		H	I	J	K
IPS e.max CAD	Crystall /Glaze	700	0	0	0.00
IPS e.max CAD-on	Fusion/ Crystall.	600	0	403	6:00
IPS e.max Press Layering Tech.	Wash firing (foundation)	0	0	0	0.00
IPS e.max Press Layering Tech.	1st/2nd Dentin/ Incisal firing	0	0	-0	0.00

*Legend

A = Standby temp.

B = Closing time.

C = Temp. increase.

D = Holding temp.

E = Holding time.

F = Vacuum on.

G = Vacuum off.

H = Long-term cooling.

I = Cool-down gradient.

J = °C.

K = mm:ss.

**<http://www.ivoclarvivadent.com/zoolu-website/media/document/4611/Programat+P300%2C+P500%2C+P700%2C+EP+3000%2C+EP+5000+-+Firing+program+tables.pdf>
<https://www.ivoclarvivadent.nl/zoolu-website/media/document/1086/Programat+CS+-+Program+Table>

TABLE III

Weibull characteristic strength and modulus

	WEIBULL CHARACTERISTIC STRENGTH	WEIBULL MODULUS
RBLDV	314.5	6.2
SFV	256.8	4.1
MLD	289.7	4.6
SLDV	305.2	5.6

TABLE IV

Paired comparison results and p-values from Weibull reliability analysis

GROUP	RBLDV	SFV	MLD	SLDV
RBLDV		0.011	0.26	0.646
SFV	RBLDV>SFV		0.174	0.036
MLD				0.490
SLDV		SFV<SLDV		

TABLE V

Shows the biaxial flexural stress (MPa) on each layer of the material at a certain load (N)

GROUP	Load (N)	Tensile Stress LD 0.55 z=0 (MPa)	Compressive Stress LD 0.5mm z=1.05 (MPa)	Compressive Stress Interface z=0.55 (MPa)
SLDV	150	221.329	221.506	10.539
	200	295.105	295.341	14.053
	250	368.882	369.177	17.566
	300	442.658	443.012	21.079
	350	516.435	516.847	24.592
	400	590.211	590.683	28.105
	450	663.987	664.518	31.618
GROUP	Load (N)	Tensile Stress LD 0.69 z=0 (MPa)	Compressive Stress LD 0.5mm z=1.19 (MPa)	Compressive Stress Interface z=0.69mm (MPa)
RBLDV	150	172.315	172.453	27.512
	200	229.753	229.937	36.683
	250	287.192	287.421	45.854
	300	344.630	344.905	55.025
	350	402.068	402.390	64.196
	400	459.507	459.874	73.367
	450	516.945	517.358	82.537
GROUP	Load (N)	Tensile Stress LD 0.7mm z=0 (MPa)	Compressive Stress FP 0.5mm z=1.2 (MPa)	Compressive Stress Interface z=0.7 (MPa)
SFV	150	172.573	169.135	30.759
	200	230.097	225.514	41.011
	250	287.621	281.892	51.264
	300	345.145	338.270	61.517
	350	402.670	394.649	71.770
	400	460.194	451.027	82.023
	450	517.718	507.405	92.276
GROUP	Load (N)	Tensile Stress LD 1.2mm (MPa)		
MLD	150	169.432		
	200	225.909		
	250	282.387		
	300	338.864		
	350	395.342		
	400	451.819		
	450	508.296		

DISCUSSION

We rejected the null hypothesis that adhering or sintering a thin laminate of LD on another LD surface would not result in increased fatigue resistance in comparison with FP on LD. This study did find a statistically significant difference between the SFV group and the two LD veneer groups, in relation to how much cyclical loading and force the specimens could survive. This result was not surprising as LD has superior mechanical properties and fracture resistance than FP.² The SFV specimens were not significantly different from the MLD specimens. A statistically significant difference was observed in the number of fragments of the RBLDV group. When the specimens fractured, they typically delaminated along the resin bond between the two layers. However, this contrasts another study, which found that the laminated group showed a decrease in the number of fragments resulting from biaxial flexural testing.²⁶ This same study found through fractographic analysis that the adhesive layer acts to deflect crack propagation through the ceramics.²⁶

A variable loading strategy was selected as it is representative of the variety of forces that may be placed upon dental restorations.³⁷ A cyclic stepwise fatigue test also seems to be more representative of a natural mastication and can help to represent the type of cyclic fatiguing that teeth and dental restorations need to endure.³⁷ This test method is designed to simulate the growth of a slow-crack starting at a critical defect.²⁹ Although simplistic in nature, this strategy is also a practical way for exploring the possible viability of a novel restorative treatment; however, further investigation would be necessary to predict actual clinical success.

For the SLDV group, reducing the size of the substructure disc in order to maintain a minimum thickness of the LD veneer was a challenge. The manufacturer's recommended thickness for the sintering porcelain used to join the LD substructure to the LD veneer is 80 micrometers. This was not achieved in this experiment with the pressure parameters that were set for the application of a 200 g weight during vibration to intimately adapt the two LD specimens together.¹⁰ The connecting porcelain layer created in this study were usually much thicker (0.15 mm) than recommended, and the substrate specimens had to be adjusted and re-polished to achieve the predetermined 1.2-mm overall thickness. Minimum thickness recommended by the manufacturer for the core is 0.8-mm thick.³⁷ The reduction in thickness from 0.7 mm to an average of 0.55 mm may have led to a reduced resistance to fracture for those specimens. A study by Anusavice et al., using finite element analysis, found 50-percent reduction in thickness of the core substructure doubled the risk of fracture for that specimen.³⁸ Other evidence suggests that not dropping the ratio of core/veneer below 1:1 was preferred.³⁷ When the ratio was 0.7 there was a significant decrease in strength, but when it was increased to 2 there was little gain beyond the 1:1 ratio.³⁷ This was used as a guideline, as none of the specimens were below this recommended 1:1 ratio. Additionally, Thompson and Rekow found that an increase in the thickness of the core structure above 0.5 mm, while the overall dimension of the core/veneer complex remained the same, had little effect on strength.³⁹

This study used an etchant and primer that are in a single bottle rather than the more historically studied hydrofluoric acid etch and silane applications. Hydrofluoric acid has traditionally been used because it etches the ceramic surface by dissolving the glassy phase and results in a roughened surface to which we can micromechanically

retain resin.⁴⁰ An important issue is the toxic nature of hydrofluoric acid and the occupational hazard it can pose to healthcare workers and patients.⁴⁰ After etching, a silane coupling agent is applied which allows a covalent bond to both resin and ceramic. A negative byproduct of this reaction is the formation of insoluble silica fluoride salts, which can interfere with the bond strength of the resin to ceramic.⁴¹ The self-etching ceramic primer was selected as various studies have shown similar results between the two processes.^{42,43} The use of ammonium polyfluoride and trimethoxypopyl methacrylate for silanization in a single bottle application was designed to be able to etch the surface while silanating in a single step application. Alrahlah et al. found that little to no etching was apparent on the surface after treatment with the self-etch ceramic primer in comparison to hydrofluoric acid; however, the same study also noted statistically insignificant bond strength differences between the two techniques.⁴³ They attributed this to the very strong bonds that can form between silica, in the ceramic, and fluoride in the ammonium polyfluoride.⁴³ Another study did find an increase in surface roughness using the same self-etch ceramic primer, and also found comparable bond strengths with aging.⁴⁰

This study reported an increase in resin performance, to a level similar to that of the sintered group. This result may be attributed to having used a different bonding protocol. Another study reported that the lamination of a material increased the strength compared to a monolithic sample.⁴⁴ Our study did not find any statistical significance between the RBLDV and SLDV group in comparison to the MLD group. Therefore, these findings could not be used to support the mentioned study (Dibner).

Lin, et al. showed that although the feldspathic specimens were weaker than the monolithic, the veneering had a stabilizing effect.¹⁴ This study, however, did not find any statistical significance of one sample group being more stable than another, using a homogeneity of variance test.

This study experimented with a novel way to gain a more favorable translucency, using CAD/CAM fabricated materials, and to use a material with higher mechanical properties in comparison with our traditional methods. Although this introductory study seems to indicate that a LD CAD/CAM fabricated veneer is comparable to MLD, and that it may be stronger than a FP hand-fabricated veneer, additional studies would be recommended prior to implementing its use in a clinical setting.

SUMMARY AND CONCLUSION

This study found that replacing the veneering substrate with LD (either resin bonded or sintered) results in an increase in fatigue resistance in comparison with using a feldspathic veneering material. It also showed that laminating the LD substructure with a LD veneer by using either attachment method (resin bonded or sintered) could return the specimens to at least a similar fracture resistance of a monolithic restoration with the same dimensions. In addition, the RBLDV group was found to break into a significantly greater number of pieces when it did fracture.

REFERENCES

1. Fasbinder DJ, Dennison JB, Heys D, Neiva G. A clinical evaluation of chairside lithium disilicate CAD/CAM crowns. *J Am Dent Assoc* 2010;141(1):10S-14S.
2. Porto TS, Roperto RC, Akkus S, et al. Effect of storage and aging conditions on the flexural strength and flexural modulus of CAD/CAM materials. *Dent Mater J* 2018;111(1):1-7.
3. Guess P, Shultheis S, Bonfante EA, Coelho PG, Ferencz JL, Silva NRFA. All-ceramic systems: laboratory and clinical performance. *Dent Clin North Am* 2011;55(2):333-52.
4. Lawson NC, Janyavula S, Syklawer S, McLaren EA, Burgess JO. Wear of enamel opposing zirconia and lithium disilicate after adjustment, polishing and glazing. *J Dent* 2014;42(12):1586-91.
5. Willard A, Chu TMG. The science and application of IPS e.Max dental ceramic. *Kaohsiung J Med Sci* 2018;34(1):238-42.
6. Hooshmand T, Parvizi S, Keshvad A. Effect of surface acid etching on the biaxial flexural strength of two hot-pressed glass ceramics. *J Prosthodont* 2008;17(5):415-9.
7. Zogheib LV, Bona AD, Kimpara ET, McCabe JF. Effect of hydrofluoric acid etching duration on the roughness and flexural strength of a lithium disilicate-based glass ceramic. *Braz Dent J* 2011;22(1):45-50.
8. Magne P, Schlichting LH, Maia HP, Baratieri LN. In vitro fatigue resistance of CAD/CAM composite resin and ceramic posterior occlusal veneers. *J Prosthet Dent* 2010;104(3):149-57.
9. E.max IPS; Clinical guide (n.d.) Retrieved from www.ivoclarvivadent.com/zoolu-website/media/document/1269/IPS+e-max+Clinical+Guide
10. Zaher AM, Hochstedler JL, Rueggeberg FA, Kee EL. Shear bond strength of zirconia-based ceramics veneered with 2 different techniques. *J Prosthet Dent* 2017;118(2):221-7.
11. Sim JY, Lee WS, Kim JH, Kim HY, Kim WC. Evaluation of shear bond strength of veneering ceramics and zirconia fabricated by the digital veneering method. *J Prosthodont Res* 2016;60(2):106-13.
12. Schmitter M, Seydler B. Minimally invasive lithium disilicate ceramic veneers fabricated using chairside CAD/CAM: A clinical report. *J Prosthet Dent* 2012;107(2):71-4.
13. Albakry M, Guazzato M, Swain MV. Biaxial flexural strength, elastic moduli, and x-ray diffraction characterization of three pressable all-ceramic materials. *J Prosthet Dent* 2003;89(4):374-80.
14. Lin WS, Ercoli C, Feng C, Morton D. The effect of core material, veneering porcelain, and fabrication technique on the biaxial flexural strength and weibull analysis of selected dental ceramics. *J Prosthodont Implant, Esthet Reconstruct Dent* 2012;21(5):353-62.
15. Höland W, Apel E, van't Hoen C, Rheinberger V. Studies of crystal phase formations in high-strength lithium disilicate glass – ceramics. *J Non-Crystalline Solid* 2006;352(38-39):4041-50
16. Chen YM, Smales RJ, Yip KHK, Sung WJ. Translucency and biaxial flexural strength of four ceramic core materials. *Dent Mater* 2008;24(11):1506-11.

17. Romanyk DL, Martinez YT, Veldhuis S, Rae N, Guo Y, Sirovica S, Fleming GJP, Addison O. Strength-limiting damage in lithium silicate glass-ceramics associated with CAD–CAM. *Dent Mater* 2019;35(1):98-104.
18. Duret F, Blouin JL, Duret B. CAD-CAM in dentistry. *J Am Dent Assoc* 1988;117(6):715-20.
19. Yao C, Zhou L, Yang H, et al. Effect of silane pretreatment on the immediate bonding of universal adhesives to computer-aided design/computer-aided manufacturing lithium disilicate glass ceramics. *European J Oral Sci* 2017;125(2):173-80.
20. Neis CA, Albuquerque NLG, Albuquerque IDS, Spazzin AO, Bacchi A. Surface treatments for repair of feldspathic, leucite-and lithium disilicate-reinforced glass ceramics using composite resin. *Braz Dent J* 2015;26(2):152-5.
21. Silva NRFA, Bonfante EA, Martins LM, et al. Reliability of reduced-thickness and thinly veneered lithium disilicate crowns. *J Dent Res* 2012;91(3):305-10.
22. Teichmann M, Gökler F, Weber V, Yildirim M, Wolfart S, Edelhoff D. Ten-year survival and complication rates of lithium-disilicate (Empress 2) tooth-supported crowns, implant-supported crowns, and fixed dental prostheses. *J Dent* 2017;56(1):65-77.
23. Zhao K, Pan Y, Guess PC, Zhang XP, Swain MV. Influence of veneer application on fracture behavior of lithium-disilicate-based ceramic crowns. *Dent Mater* 2012;28(6):653-60.
24. Jian Y, He ZH, Dao L, Swain MV, Zhang XP, Zhao K. Three-dimensional characterization and distribution of fabrication defects in bilayered lithium disilicate glass-ceramic molar crowns. *Dent Mater* 2017;33(4):e178-e185.
25. Wattanasirmkit K, Srimaneepong V, Kanchanatawewat K, Monmaturapoj N, Thunyakitpisal P, Jinawath S. Improving shear bond strength between feldspathic porcelain and zirconia substructure with lithium disilicate glass-ceramic liner. *Dent Mater J* 2015;34(3):302-9.
26. Costa AKF, Kelly RD, Fleming GJP, Borges ALS, Addison O. Laminated ceramics with elastic interfaces: A mechanical advantage? *J Dent* 2015;43(3):335-41.
27. Campos F, Valandro LF, Feitosa SA, et al. Adhesive cementation promotes higher fatigue resistance to zirconia crowns. *Operative Dent* 2017;42(2):215-24.
28. Kawewongprasert P, Phasuk K, Levon JA, et al. Fatigue failure load of lithium disilicate restorations cemented on a chairside titanium base. *J Prosthodont* 2018;00(1):1-9.
29. Madruga CFL, Bueno MG, Dal Piva AMO, et al. Sequential usage of diamond bur for CAD/CAM milling: Effect on the roughness, topography and fatigue strength of lithium disilicate glass ceramic. *J Mechanic Behavior Biomed Mater* 2019;91(1):326-34.
30. Beuer F, Schweiger J, Eichberger M, Kappert HF, Gernet W, Edelhoff D. High-strength CAD/CAM-fabricated veneering material sintered to zirconia copings – a new fabrication mode for all-ceramic restorations. *Dent Mater* 2009;25(1):121-8.
31. Chi WJ, Browning W, Looney S, Mackert JR, Windhorn RJ, Rueggeberg F. Resistance to abrasion of extrinsic porcelain esthetic characterization techniques. *US Army Med Department J* 2017;July-Sep:71-79.

32. Costa AKF, Borges ALS, Fleming GJP, Addison O. The strength of sintered and adhesively bonded zirconia/veneer-ceramic bilayers. *J Dent Mater* 2014;42(10):1269-76.
33. Anami LC, Lima JMC, Valandro LF, Kleverlaan CJ, Feilzer AJ, Bottino MA. Fatigue resistance of Y-TZP/porcelain crowns is not influenced by the conditioning of the intaglio surface. *Operative Dent* 2016;41(1):E1-E2.
34. Schmitter M, Schweiger M, Mueller D, Rues S. Effect on in vitro fracture resistance of the technique used to attach lithium disilicate ceramic veneer to zirconia frameworks. *Dent Mater* 2014;30(2):122-30.
35. Sawada T, Schille C, Wagner V, Spintzyk S, Schweizer E, Geis-Gerstorfer J. Biaxial flexural strength of the bilayered disk composed of ceria-stabilized zirconia/alumina nanocomposite (Ce-TZP/A) and veneering porcelain. *Dent Mater* 2018;34(8):1199-1210.
36. Hsueh CH, Luttrell CR, Becher PF. Analyses of multilayered dental ceramics subjected to biaxial flexure tests. *Dent Mater* 2006;22(5):460-9.
37. Nawafleh N, Hatamleh MM, Öchsner A, Mack, F. The impact of core/veneer thickness ratio and cyclic loading on fracture resistance of lithium disilicate crown. *J Prosthodont* 2018;27(1):75-82.
38. Anusavice KJ, Jadaan OM, Esquivel-Upshaw JF. Time-dependent fracture probability of bilayer, lithium-disilicate-based, glass-ceramic, molar crowns as a function of core/veneer thickness ratio and load orientation. *Dent Mater* 2013;29(1):1132-8.
39. Thompson VP, Rekow DE. Dental ceramics and the molar crown testing ground. *J Applied Oral Sci* 2004;12(SPE):26-36.
40. Tribst JPM, Anami LC, Özcan M, Bottino, M, Melo RM, Saavedra GSFA. Self-etching primers vs acid conditioning: impact on bond strength between ceramics and resin cement. *Operative Dent* 2018;43(4):372-9.
41. Fabianelli A, Pollington S, Papacchini F, et al. The effect of different surface treatments on bond strength between leucite reinforced feldspathic ceramic and composite resin. *J Dent* 2010;38(1):39-43.
42. Al-Harhi AA, Aljoudi MH, Almaliki MN, El-Banna KA. Laboratory study of micro-shear bond strength of two resin cements to leucite ceramics using different ceramic primers. *J Contemporary Dent Pract* 2018;19(8):918-24.
43. Alrahlah A, Awad MM, Vohra F, Al-Mudahi A, Al Jeaidi, ZA, Elsharawy M. Effect of self-etching ceramic primer and universal adhesive on bond strength of lithium disilicate ceramic. *J Adhesion Sci Technol* 2017;31(23):2611-9.
44. Dibner AC, Kelly JR. Fatigue strength of bilayered ceramics under cyclic loading as a function of core veneer thickness ratios. *J Prosthet Dent* 2016;115(3):335-40.
45. Kern M, Sasse M, Wolfart S. Ten-year outcome of three-unit fixed dental prostheses made from monolithic lithium disilicate ceramic. *J Am Dent Assoc* 2012;143(3):234-40.
46. Programat - Firing Program Table (n.d.) Retrieved from <https://www.ivoclarvivadent.com/zooluwebsite/media/document/4611/Programat+P300%2C+P500%2C+P700%2C+EP+3000%2C+EP+5000+-+Firing+program+table>

47. Özcan M, Vallittue PK. Effect of surface conditioning methods on the bond strength of luting cement to ceramics. *Dent Mater* 2003;19(8):725-31.
48. Borges GA, Sophyr AM, De Goes MF, Sobrinho, LC, Chan DC. Effect of etching and airborne particle abrasion on the microstructure of different dental ceramics. *J Prosthet Dent* 2003;89(5):479-88.
49. Bitter K, Paris S, Hartwig C, Neumann K, Kielbassa AM. Shear bond strengths of different substrates bonded to lithium disilicate ceramics. *Dent Mater J* 2006;25(3):493-502.
50. Akgungor G, Akkayan B, Gaucher, H. Influence of ceramic thickness and polymerization mode of a resin luting agent on early bond strength and durability with a lithium disilicate-based ceramic system. *J Prosthet Dent* 2005;94(3):234-41.
51. Schlichting LH, Maia HP, Baratieri LN, Magne P. Novel-design ultra-thin CAD/CAM composite resin and ceramic occlusal veneers for the treatment of severe dental erosion. *J Prosthet Dent* 2011;105(4):217-26.
52. Choi YS, Kim SH, Lee JB, Han JS, Yeo IS. In vitro evaluation of fracture strength of zirconia restoration veneered with various ceramic materials. *J Advanced Prosthodont* 2012;4(3):162-9.
53. Schmitter M, Mueller D, Rues S. Chipping behaviour of all-ceramic crowns with zirconia framework and CAD/CAM manufactured veneer. *J Dent* 2012;40(2):154-62.
54. Silva NR, Thompson VP, Valverde GB, etc. Comparative reliability analyses of zirconium oxide and lithium disilicate restorations in vitro and in vivo. *J Am Dent Assoc* 2011;142(2):4S-9S.
55. Zhao K, Wei YR, Pan Y, Zhang XP, Swain MV, Guess PC. Influence of veneer and cyclic loading on failure behavior of lithium disilicate glass-ceramic molar crowns. *Dent Mater* 2014;30(2):64-171.
56. Gehrt M, Wolfart S, Rafai N, Reich S, Edelhoff D. Clinical results of lithium-disilicate crowns after up to 9 years of service. *Clin Oral Investig* 2013;17(1):275-84.
57. Carvalho AA, Moreira FDCL, Fonseca RB, et al. Effect of light sources and curing mode techniques on sorption, solubility and biaxial flexural strength of a composite resin. *J Applied Oral Sci* 2012;20(2):246-52.
58. Guarda GB, Correr, AB, Goncalves LS, et al. Effects of surface treatments, thermocycling, and cyclic loading on the bond strength of a resin cement bonded to a lithium disilicate glass ceramic. *Operative Dent* 2013;38(2):208-17.
59. Guess, PC Schultheis S, Wolkewitz M, Zhang Y, Strub JR. Influence of preparation design and ceramic thicknesses on fracture resistance and failure modes of premolar partial coverage restorations. *J Prosthet Dent* 2013;110(4):264-73.
60. Magne P, Carvalho AO, Bruzi G, Giannini M. Fatigue resistance of ultrathin CAD/CAM complete crowns with a simplified cementation process. *J Prosthet Dent* 2015;114(4):574-9.

61. Sailer I, Makarov NA, Thoma DS, Zwahlen M, Pjetursson BE. All-ceramic or metal-ceramic tooth-supported fixed dental prostheses (FDPs)? A systematic review of the survival and complication rates. (Pt 1). Single crowns (SCs). *Dent Mater* 2015;31(6):603-23.
62. Kassardjian V, Varma S, Andiappan M, Creugers NH, Bartlett D. A systematic review and meta-analysis of the longevity of anterior and posterior all-ceramic crowns. *J Dent* 2016;55(1):1-6.
63. Clausen JO, Tara MA, Kern M. Dynamic fatigue and fracture resistance of non-retentive all-ceramic full-coverage molar restorations. Influence of ceramic material and preparation design. *Dent Mater* 2010;26(6):533-8.
64. Aboushelib MN, De Jager N, Kleverlaan CJ, Feilzer AJ. Microtensile bond strength of different components of core veneered all-ceramic restorations. *Dent Mater* 2005;21(10):984-91.
65. Nishigori A, Yoshida T, Bottino MC, Platt JA. Influence of zirconia surface treatment on veneering porcelain shear bond strength after cyclic loading. *J Prosthet Dent* 2014;112(6):1392-8.
66. Guess PC, Zavanelli RA, Silva NR, Bonfante EA, Coelho PG, Thompson VP. Monolithic CAD/CAM lithium disilicate versus veneered Y-TZP crowns: comparison of failure modes and reliability after fatigue. *Int J Prosthodont* 2014;23(5):434-42.

ABSTRACT

STEPWISE STRESS TESTING OF DIFFERENT CAD/CAM LITHIUM-DISILICATE
VENEER APPLICATION METHODS TO LITHIUM-DISILICATE
SUBSTRUCTURE

by

Jaren Thomas May

Indiana University School of Dentistry
Indianapolis, Indiana

Objective: CAD/CAM technology allows fabrication of thin lithium disilicate (LD) veneers to a LD crown substructure in place of using traditional feldspathic porcelain (FP) which has inferior mechanical properties. This project investigated the effect of different LD veneer applications to LD substructure on the biaxial flexural fatigue of LD veneer/substructure restorations.

Materials/Methods: Forty-five LD discs ($\varnothing = 12 \times 0.7$ mm) were fabricated that, when combined with the veneering discs, achieve final dimensions of ($\varnothing = 12 \times 1.2$ mm). Experimental groups were ($n = 15$) as follows: (1) Resin Bonded LD Veneer (RBLDV), LD veneer ($\varnothing = 12 \times 0.5$ mm) adhesively cemented to LD (0.7 mm); (2) Sintered LD Veneer (SLDV), LD veneer ($\varnothing = 12 \times 0.5$ mm) sintered to LD (0.7 mm); (3) Sintered Feldspathic Veneer (SFV), feldspathic porcelain (FP) applied to LD discs to achieve a

final dimension of ($\emptyset = 12 \times 1.2$ mm). A fourth group of (1.2 mm) monolithic LD served as the control. Weibull-distribution survival analysis was used to compare the differences of the resistance to fracture after fatigue between groups. Total number of cycles were analyzed using one-way Anova ($p < 0.05$).

Hypothesis: Adhering or sintering a thin laminate layer of LD on another LD surface would result in increased fracture resistance in comparison to sintered FP on LD.

Results: The SFV group had significantly lower fatigue resistance than SLDV and RBLDV groups ($p < 0.05$). The RBLDV group fractures resulted in significantly more fractured fragments in comparison to the other groups. No statistical difference was observed in the number of cycles. The results also showed that the LD veneered groups presented similar resistance to fatigue as monolithic discs of the same overall dimensions.

Conclusion: The hypothesis was accepted suggesting that veneering a LD substructure with a LD veneer, bonded or sintered, has increased resistance to fatigue as FP veneering material on a LD substructure. In addition, it was observed to have similar resistance to fatigue in comparison to the monolithic LD group.

CURRICULUM VITAE

Jaren T. May

July 15, 1982	Born in Payson, UT
May 2007	BS Brigham Young University Provo, UT
May 2011	DDS The University of Oklahoma College of Dentistry Oklahoma City, Oklahoma
July 2011 to July 2012	Advanced Education in General Dentistry Residency Norfolk Naval Base Norfolk, VA
July 2012 to 2014	Dental Division Officer USS Theodore Roosevelt, CVN-71 Norfolk, VA
July 2014 to 2016	Dental Officer Parris Island Marine Recruit Depot Parris Island, SC
July 2016 to 2019	Operative Dentistry Residency Indiana University School of Dentistry Indianapolis, IN

Professional Organizations

Fellow in the Academy of General Dentistry
Academy of Operative Dentistry
American Dental Association
Academy of Cosmetic Dentistry (Seeking accreditation status)
Past President and Secretary, Low Country Dental Study Club (2014 to 2016)